ASM | mBio

| Editor's Pick | Host-Microbial Interactions | Research Article

Spatiotemporal compartmentalization of NADPH oxidase signaling coordinates cell fusion and predatory behavior in nematode-trapping fungi

Marius Kriegler,[1] Valentin Wernet,[1] Satur Herrero,[1] Reinhard Fischer[1]

AUTHOR AFFILIATION See affiliation list on p. 16.

ABSTRACT Reactive oxygen species (ROS) act both as cytotoxic agents and essential signaling molecules. In the nematode-trapping fungus *Arthrobotrys flagrans*, we investigated how ROS coordinate the development and function of adhesive trapping networks used to capture *Caenorhabditis elegans*. We demonstrate a distinct functional specialization between the two NADPH oxidases NoxA and NoxB, which are both activated by the regulatory subunit NoxR. The NoxB-NoxR complex was specifically active in trap cells, where it was required for producing the adhesive "glue" for prey capture. In contrast, NoxA localized to the plasma membrane of vegetative hyphae and was required for hyphal fusion and trap closure. NoxA was activated by the pulsatile recruitment of NoxR to the hyphal tip, suggesting oscillatory ROS production during hyphal expansion and hyphal fusion. Nox complexes initially generate superoxide, which is probably converted to more stable hydrogen peroxide (H_2O_2) and serves as a key spatial signal. Together, these findings reveal a remarkable division of labor between Nox isoforms, where spatial compartmentalization of ROS signaling drives fungal morphogenesis and predatory behavior.

IMPORTANCE Reactive oxygen species (ROS) are not only toxic byproducts of mitochondrial activity but also important signaling molecules in eukaryotes. To fulfill this signaling role, ROS production must be tightly regulated. NADPH oxidases are key contributors to controlled ROS generation, as they may be regulated at the transcriptional level, targeted to specific cellular locations, and activated by dedicated regulatory proteins. Here, we investigated the role of NADPH oxidases in the nematode-trapping fungus Arthrobotrys flagrans and show that two NADPH oxidases serve distinct roles: one is required for trap function, while the other mediates cell-to-cell communication and is required for hyphal fusion and trap closure. The latter finding suggests ROS, most likely H_2O_2, as a diffusible signaling molecule between communicating fungal cells.

KEYWORDS NADPH-oxidases, nematode trapping, ROS, cell fusion, cell communication, Arthrobotrys

Reactive oxygen species (ROS), including superoxide anions (O_2^-), hydrogen peroxide (H_2O_2), and hydroxyl radicals (•OH), are ubiquitous signaling molecules in eukaryotic organisms (1, 2). Although traditionally regarded as damaging byproducts of aerobic metabolism, ROS are now recognized as crucial signaling molecules that regulate diverse cellular processes, including development, stress responses, and host-pathogen interactions (3, 4). The spatial and temporal control of ROS production is essential, as imbalances can lead to oxidative stress and cellular dysfunction (5).

Although the mitochondrial respiratory chain is a major source of ROS, eukaryotic cells also produce ROS actively through specialized enzymes known as NADPH oxidases

Editor Erika Kothe, Friedrich-Schiller-Universitat, Jena, Germany

Address correspondence to Reinhard Fischer, reinhard.fischer@kit.edu.

The authors declare no conflict of interest.

See the funding table on p. 16.

Received 15 June 2026
Accepted 23 June 2026
Published 15 July 2026

(Nox) (6). These membrane-associated, heme-containing flavocytochromes catalyze the transfer of electrons from cytosolic NADPH to molecular oxygen, generating superoxide, which is converted to more stable ROS like hydrogen peroxide (7). In animals, Nox-derived ROS regulate processes such as immune defense, cell proliferation, and apoptosis (8). In plants, they act as key messengers in development, stress responses, and pathogen defense (9). In root hairs, oscillatory feedback loops between Ca^{2+} and ROS regulate tip growth and cell wall expansion (10). Beyond localized signaling, ROS have been identified as mediators of long-distance communication. In zebrafish, for instance, tissue-scale gradients orchestrate leukocyte recruitment to injury sites (11). In plants, a ROS wave mechanism was shown where ROS produced by one cell's NADPH oxidase triggers production in neighboring cells, enabling systemic stress signaling across the entire organism (12).

In fungi, three subfamilies of Nox proteins are distinguished: NoxA, NoxB, and NoxC (13). NoxA and NoxB are structurally similar to the mammalian $gp91^{phox}$, whereas NoxC is more rarely found and contains a characteristic EF-hand calcium-binding domain, resembling the plant Rboh (respiratory burst oxidase homologs) family (14). Like the human activator $p67^{phox}$, the fungal NoxR protein functions as an essential activator of the Nox complex (15). Additional regulatory proteins include the guanine nucleotide exchange factor Cdc24, the small GTPase Rac, and the scaffold protein Bem1 (16, 17). Furthermore, NoxA interacts with the membrane protein Ham6, while NoxB requires Pls1 (18–20). Deletion of *ham6* or *plsA* results in phenotypes that partially overlap with those observed in *nox*-deletion mutants. In *Botrytis cinerea*, deletion of *plsA*, in contrast to *noxB*, was found to impair female fertility but not ascospore germination. Furthermore, *plsA* deletion did not affect ROS production (21).

Phylogenetic analyses suggest that most fungal species possess two distinct NADPH oxidases, NoxA and NoxB. In several filamentous fungi, such as *Magnaporthe oryzae*, *Botrytis cinerea*, and *Verticillium dahliae*, both NoxA and NoxB are crucial for plant virulence (18, 21–24). Corresponding deletion mutants show defects in appressorium formation and penetration of plant tissues. It has been demonstrated that Nox activity is required for the proper assembly of the actin-septin ring at the penetration site (24). In addition to their roles in pathogenicity, Nox proteins are also involved in spore development, apical dominance, cell fusion, mutualistic interactions, and oxidative stress resistance (25–28). Unicellular yeasts were long believed not to use Nox proteins. However, an intracellular Nox enzyme, Yno1, has been identified in *Saccharomyces cerevisiae* and shown to generate intracellular ROS, which are thought to play important roles in apoptosis and cytoskeletal regulation (29, 30). In *Candida albicans*, by contrast, the ferric reductase Fre8 is strongly induced during hyphal growth, and the resulting ROS production is essential for morphogenesis and virulence (31). Unlike classical Nox enzymes, these yeast ROS-generating enzymes do not require a NoxR activator.

Nematode-trapping fungi comprise a unique group of ascomycetes, basidiomycetes, and zygomycetes that are capable of forming specialized trapping structures to capture nematodes (32). Under nutrient-rich conditions, these fungi typically grow saprotrophically and do not develop traps, thereby avoiding the energetic costs associated with trap formation. In contrast, nutrient limitation, particularly nitrogen starvation, combined with the presence of nematodes or nematode-derived signals, induces the development of trapping structures. These traps display distinct cellular characteristics compared to vegetative hyphae (32). *Arthrobotrys flagrans* (formerly *Duddingtonia flagrans*), an ascomycete, produces adhesive ring-shaped traps that enable the efficient capture of nematodes (33). The fungus forms a fluffy mycelium consisting of aerial hyphae, which are interconnected through extensive hyphal fusion, resulting in a highly integrated mycelial network. Reproduction occurs through the production and dispersal of conidia and chlamydospores, whereas a sexual stage has not yet been reported. Through long-term co-evolution between predator and prey, fungi like *A. flagrans* have evolved specialized virulence factors and metabolites to lure nematodes into these traps and facilitate their digestion (34–38). To regulate trap morphogenesis, nematode-trapping

fungi utilize specialized G-protein-coupled receptors that sense nematode-derived molecules and modulate downstream signaling pathways (39, 40). The trap formation process requires special polarity markers like the cell-end marker proteins to bend the trap into a ring shape (41, 42). Formation of a complete trap requires somatic cell fusion at the ends of the trap. This process is coordinated through a so-called "ping-pong" communication mechanism or dialog, in which interacting cells alternately act as signal senders and receivers (43–45). Previous studies have shown that reactive oxygen species play an important role in this process (25). In *Arthrobotrys oligospora*, ROS were demonstrated to function as trap-inducing signals, and deletion of *noxA* resulted in a reduced number of traps compared to the wild type (46).

In this study, we investigated the role of NADPH oxidases in *A. flagrans* and showed that NoxA and NoxB fulfill distinct biological functions. While NoxA is specifically required for somatic cell fusion and trap closure, NoxB is essential for trap functioning.

RESULTS

The NADPH-oxidase NoxA and the activator NoxR are required for cell fusion

Fungal Nox proteins share the typical structural features of the family, including six transmembrane helices, two FAD-binding, and two NADPH-binding domains (14). To identify Nox components in *A. flagrans*, BLAST searches were performed using homologs from other fungal species. NoxA (DFL_005041), NoxB (DFL_009580), NoxR (DFL_001795), and PlsA (Pls1) (DFL_002727) were identified in *A. flagrans*, all of which exhibit the characteristic domain architecture (Fig. 1A and B). NoxB is slightly larger than NoxA due to a small N-terminal extension. The Nox activator NoxR contains several tetratricopeptide repeats (TPRs), as well as a PB1 domain that mediates protein-protein interactions. The tetraspanin Pls1, which interacts with NoxB at the membrane, contains four transmembrane domains (23). In addition, two NoxR-like proteins (DFL_008703; DFL_002559) were detected, showing high overall similarity to NoxR but possessing a slightly divergent Nox-activation domain.

To investigate the role of Nox proteins in *A. flagrans*, deletion mutants of *noxA*, *noxB*, *plsA*, and *noxR* were generated via homologous recombination, along with the corresponding recomplemented strains. On solid medium, only the *noxA* and *noxR* mutants displayed a visible phenotype (Fig. 1C). While the WT forms aerial hyphae, resulting in a fluffy colony morphology, the Δ*noxA* and Δ*noxR* strains exhibited a flat colony surface. The lack of aerial mycelium resembles hyphal-fusion mutants (47). In contrast, the Δ*noxB* and Δ*plsA* strains still produced extensive aerial hyphae similar to the WT. Indeed, both Δ*noxA* and Δ*noxR* strains were unable to undergo hyphal fusion. Although *A. flagrans* usually performs frequent cell-cell fusions within the colony, the defect was most evident in trap morphology. Traps were induced on low-nutrient agar in the presence of nematodes. In the wild type, most traps re-fuse at the ends of the rings, forming closed three-dimensional loops. In contrast, traps of the Δ*noxA* and Δ*noxR* mutants never underwent fusion, resulting in open, screw-like structures (Fig. 1C). The Δ*noxB* and Δ*plsA* strains did not display any hyphal-fusion phenotype. Therefore, we next analyzed the functionality of the traps in virulence assays.

NoxB, NoxR, and PlsA are required for effective nematode trapping

In the first attempts to evaluate the trapping efficacy of the traps in the different mutants, it became apparent that the Δ*noxB*, Δ*plsA*, and Δ*noxR* mutants contained a higher proportion of empty traps compared to the wild-type and the *noxA*-deletion strain. Captured large nematodes were rarely observed in these mutants. Therefore, an assay was performed to quantify the effect. First, nematodes were synchronized to ensure uniform sizes. *A. flagrans* was grown on low-nutrient medium (LNM) agar, and trap formation was induced by adding a mixed nematode population. The following day, nematodes were washed off the pads, and 0.25 cm^2 agar pads containing the fungal mycelium and traps were excised. Approximately 150 synchronized nematodes were

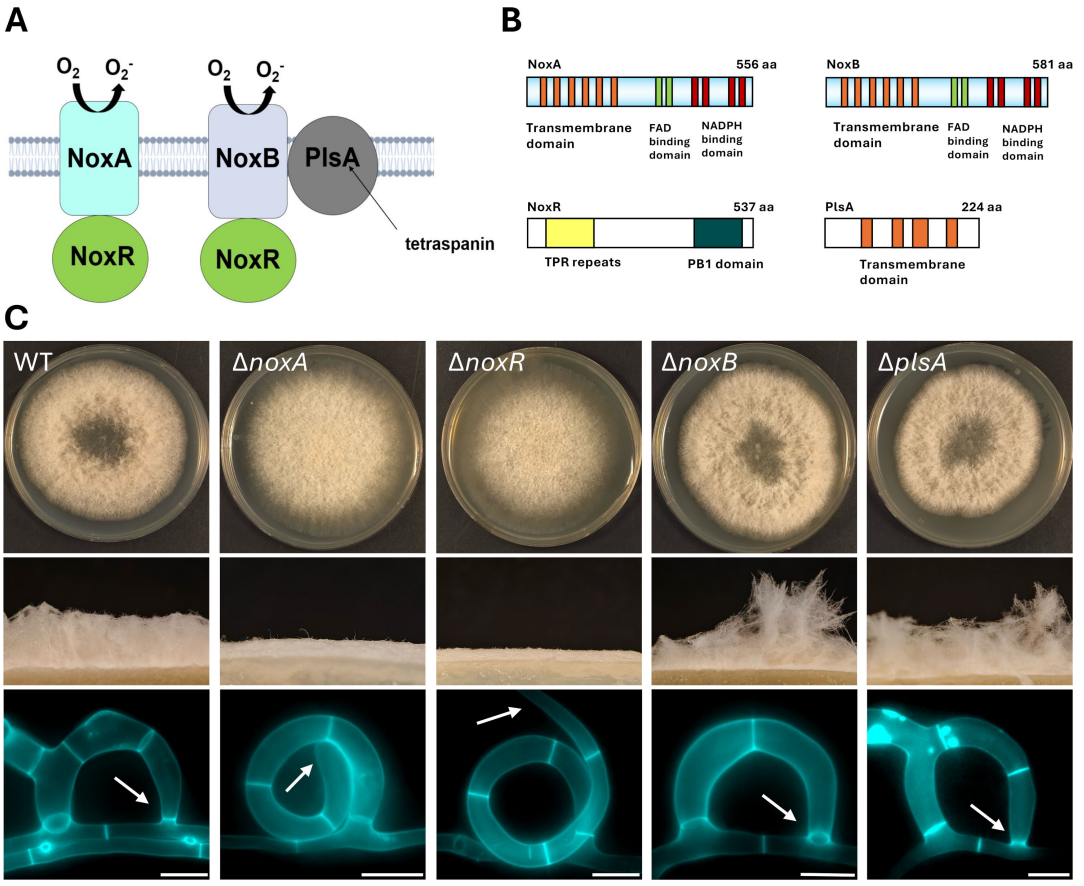

FIG 1 Only the NoxA-NoxR complex is required for hyphal fusion and trap formation. (A) Simplified model of the NADPH oxidase complexes NoxA and NoxB. NoxA and NoxB interact with the regulatory subunit NoxR to produce superoxide (O_2^-). PlsA is a tetraspanin/transmembrane protein that specifically interacts with NoxB. (B) Domain architecture of the Nox components NoxA, NoxB, NoxR, and PlsA. Transmembrane domains (orange), FAD-binding domains (green), NADPH-binding domains (red), TPR domains (yellow), and the PB1 domain (blue) are indicated. (C) Phenotypic characterization of colony growth, aerial hyphae, and trap formation. Top row: colony morphology on potato dextrose agar (PDA) plates after 6 days of incubation. Colony diameter was unchanged. However, Δ*noxA* and Δ*noxR* strains exhibited reduced aerial hyphae. Middle row: side view of aerial hyphae. Δ*noxA* and Δ*noxR* colonies remained flat compared to WT, Δ*noxB*, and Δ*plsA* strains. Bottom row: trap formation on low-nutrient medium (LNM) induced with a mixed population of nematodes. WT, Δ*noxB,* and Δ*plsA* formed normal traps that closed via hyphal fusion, whereas Δ*noxA* and Δ*noxR* strains were defective in hyphal fusion, resulting in open traps. Scale bar: 10 µm.

then applied to each pad. After 30 min, the number of empty traps and traps containing a nematode was recorded. Time-lapse videos of the capture process were taken using a stereomicroscope (Movies S1 to S3).

The wild type rapidly captured nematodes, and after 30 min, a large number of animals were caught in the traps (Fig. 2A and B). Approximately half of the traps contained a nematode. The Δ*noxA* strain, despite its altered trap morphology, captured only slightly fewer nematodes compared to the WT. In contrast, the Δ*noxB*, Δ*noxR*, and Δ*plsA* strains exhibited a pronounced defect in trapping efficiency and were nearly incapable of restraining larger nematodes. Although some traps contained small nematodes, which were used for trap induction the day before, indicating that the mutants are still capable of capturing and colonizing nematodes, the videos revealed that larger nematodes frequently escaped from the traps after initially being caught (Fig. 2C). These observations suggest that traps formed by the Δ*noxB*, Δ*noxR*, and Δ*plsA* strains possess reduced adhesive strength: sufficient to retain small nematodes, but not sufficient to effectively restrain larger prey.

In *Magnaporthe grisea*, deletion of Nox proteins has been shown to impair formation of the actin-septin ring required for host penetration (24). To confirm whether a similar mechanism works in *A. flagrans*, we tagged the septin Cdc10 with mCherry

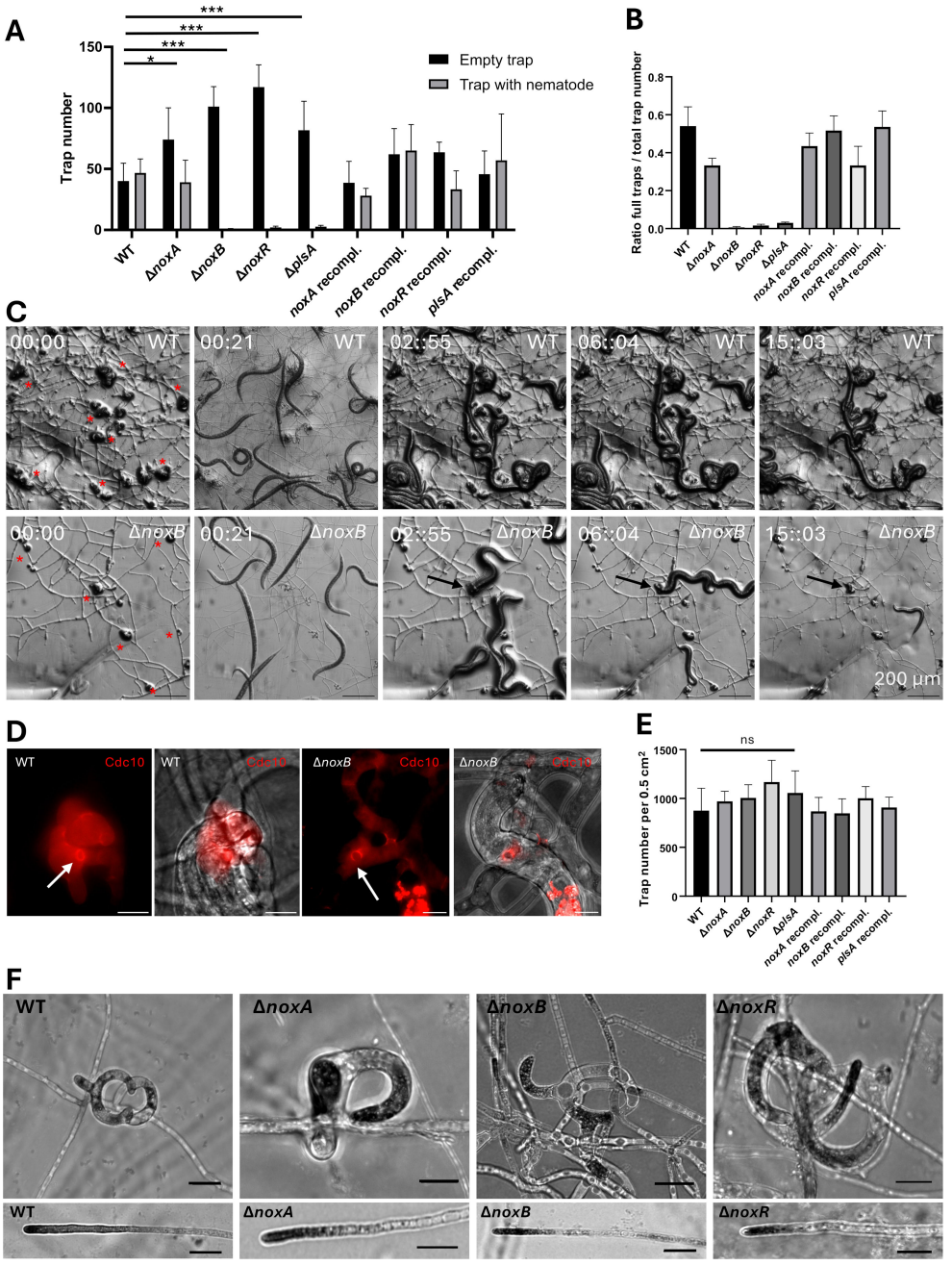

FIG 2 The NoxB-NoxR complex is required for trap functionality. (A, B) The WT and Δ*noxA*, Δ*noxB*, Δ*plsA,* and Δ*noxR* strains were grown on LNM media, and the traps were induced with a mixed population of nematodes. After 1 day, the nematodes were washed off, and a synchronized population of L4 nematodes was put on a 0.25 mm^2 excised block of LNM for each respective strain. Traps containing a nematode and empty traps were quantified after 30 min. The Δ*noxA* mutant exhibited a slight reduction in trapping efficiency, whereas Δ*noxB*, Δ*plsA,* and Δ*noxR* strains showed a severe reduction in trapping efficiency compared to WT. $n = 3$. (C) Time-lapse imaging of nematode capture by WT and Δ*noxB* strains. Red asterisks indicate empty traps; arrows mark captured nematodes that subsequently escape after several minutes. WT efficiently captured nematodes within a short time frame, while Δ*noxB* was incapable of capturing adult nematodes. Scale bar: 200 µm. (D) The septin Cdc10 forms a ring at the nematode penetration site. Both WT and Δ*noxB* strains formed intact septin rings and successfully penetrated captured nematodes. Scale bar = 10 µm. (E) Analysis of trap formation after 1 day of incubation with nematodes on LNM. No significant differences in trap numbers were observed among the strains. (F) ROS visualization by nitro blue tetrazolium chloride (NBT) staining. Data are presented as mean ± s.d. *$P < 0.05$; **$P < 0.01$; ***$P < 0.001$; ****$P < 0.0001$; ns, not significant (two-tailed unpaired *t*-test).

and ectopically integrated the construct into the WT and Δ*noxB* strains (Fig. 2D). Upon nematode capture, both strains displayed a distinct ring-shaped Cdc10 signal at the penetration site. Thus, we found no evidence that actin-septin ring formation is compromised in the Δ*noxB* strain.

Notably, quantification of trap formation after nematode induction revealed no significant change in the deletion strains compared to the WT (Fig. 2E). The Δ*noxR* strain even showed slightly higher trap numbers than the WT. This contrasts with observations in *A. oligospora*, where deletion of *noxA* results in reduced trap numbers compared to WT (46). These findings indicate that, despite their close relatedness, the two species exhibit molecular differences in the regulation of trap development.

To assess ROS production in the different strains, we used nitro blue tetrazolium chloride (NBT) staining, which forms a dark violet precipitate upon oxidation. After 30 min of incubation, increased staining was observed in traps and at hyphal tips in WT (Fig. 2F). The same staining pattern was also detected in all mutant strains. The absence of detectable differences between the WT and the *nox*-deletion strains has also been reported in other fungal species and suggests the presence of additional ROS-producing mechanisms that contribute significantly to extracellular ROS levels (21, 48). After the description of the very distinct phenotypes of the *noxA*- and the *noxB*-deletion strains, we aimed at explaining the phenotypes at the molecular level.

Distinct gene sets are regulated by NoxA and NoxB

To further investigate the roles of NoxA and NoxB in *A. flagrans*, an RNA-seq analysis was performed. Three biological replicates of the WT, Δ*noxA,* and Δ*noxB* strains, which were induced with nematodes, were pooled and processed for RNA sequencing.

In the Δ*noxA* strain, 1,119 genes were upregulated and 948 genes were downregulated relative to the WT. In the Δ*noxB* strain, 371 genes were upregulated and 303 were downregulated (Fig. S1A and B and S2). Enrichment analysis revealed that both mutants displayed significant alterations in genes associated with carbohydrate metabolism (Fig. S1C). Notably, the Δ*noxB* mutant showed a specific enrichment in pathogenesis-related genes, a pattern not observed in the *noxA*-deletion strain.

noxB and *plsA* are upregulated during trap formation, while *noxA* is downregulated

As a first step to understand the role of NoxA and NoxB in trap morphogenesis and trap functioning, we analyzed the expression of *noxA, noxB, noxR,* and *plsA* using a promoter-reporter assay. To this end, the respective promoters were fused to a *histone(h2b)-mCherry* construct, resulting in fluorescently labeled nuclei if the promoters are active. Targeting of the fluorescent protein to nuclei prevents misinterpretations due to autofluorescence in the cytoplasm. Hence, the fluorescent signal intensity in nuclei reflects promoter activity in the corresponding cellular regions (Fig. 3A). As a control for constitutive expression, the *h2b* promoter was fused to a *histone-GFP* open reading frame. Fluorescence microscopy revealed that *noxB* and *plsA* promoters were strongly activated in traps and in the surrounding hyphal regions. In contrast, *noxA* and *noxR* promoters were also highly active in vegetative hyphae in the absence of nematodes. Fluorescence in vegetative hyphae was not obvious if, in the observed area, highly fluorescent traps were present and the exposure time was adjusted to the trap fluorescence. Therefore, we selected a round area away from a trap and increased the brightness of that area until the fluorescence of nuclei became apparent. Quantification of nuclear fluorescence (n = 75 nuclei) in traps and trap-free mycelium confirmed these observations. Nuclei within traps exhibited markedly higher fluorescence in the *noxB* and *plsA* promoter fusion strains, whereas fluorescence in vegetative hyphae was barely detectable. In contrast, the *noxA* and *noxR* promoter fusions showed no significant difference in nuclear fluorescence between trap and non-trap regions, with nuclei remaining readily visible in both tissues (Fig. 3B).

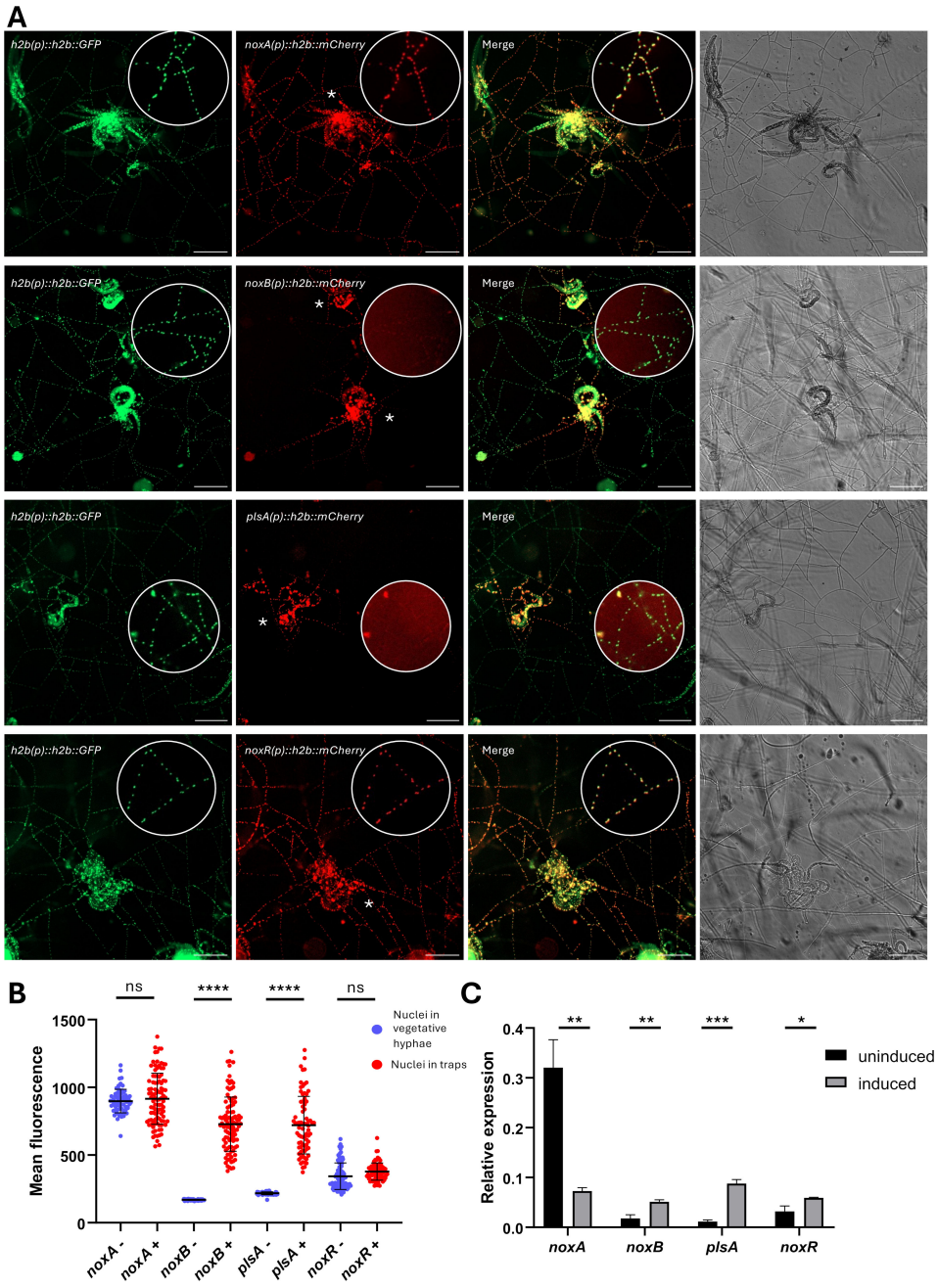

FIG 3 The *noxA* gene is expressed in hyphae, whereas the *noxB* gene is upregulated in traps. (A) Fluorescence microscopy of strains expressing *h2b(p)::h2b::GFP* as a constitutive control and *h2b::mCherry* under the control of the *noxA*, *noxB*, *plsA*, or *noxR* promoters. Asterisks indicate trap structures, and white circles highlight magnified regions lacking traps. In vegetative hyphae, nuclei were barely detectable in strains carrying the *noxB* and *plsA* promoter fusions, whereas strong nuclear fluorescence was observed in traps. Scale bar = 200 µm. (B) Quantification of mean fluorescence intensity for the indicated promoter constructs. Blue dots represent nuclei in vegetative hyphae, and red dots represent nuclei in traps. *noxB* and *plsA* promoters exhibited significantly higher fluorescence in traps compared to *noxA* and *noxR* promoters. $n = 75$ nuclei. (C) Relative gene expression levels of *noxA*, *noxB*, *plsA,* and *noxR* measured by RT-qPCR under uninduced (black) and nematode-induced (gray) conditions ($n = 3$). *noxA* is downregulated, while *noxB*, *plsA,* and *noxR* are upregulated during trap formation. Data are presented as mean ± s.d. *$P < 0.05$; **$P < 0.01$; ***$P < 0.001$; ****$P < 0.0001$; ns, not significant (two-tailed unpaired *t*-test).

To further quantify gene-expression levels, qPCR analyses were performed using wild-type cultures grown on LNM for 2 days, either with or without nematodes (Fig. 3C).

The experiment was conducted in three biological replicates. Relative expression of *noxA*, normalized to the housekeeping gene *h2b*, decreased during trap formation from 0.32 (±0.06) in uninduced cultures to 0.073 (±0.007) upon nematode induction. In contrast, *noxB* expression significantly increased from 0.018 (±0.007) in uninduced cultures to 0.05 (±0.0044) under induced conditions. Expression of *plsA* also increased from 0.012 (±0.0033) in the control to 0.09 (±0.008) during trap induction, whereas *noxR* exhibited a moderate increase from 0.03 (±0.01) to 0.06 (±0.014). In conclusion, both *noxB* and *plsA* were upregulated during trap formation, consistent with their trap-localized promoter activity. *noxR* displayed a small increase in expression, although the promoter-fusion assay did not show a clear induction, likely due to promoter activity already being high in vegetative hyphae, reducing the detectable dynamic range. *noxA* was the only gene that showed no evidence of upregulation in either the promoter fusion or the qPCR assay.

NoxA localizes at the membrane of vegetative hyphae, while NoxB and PlsA localize in vesicles at the inner rim of traps

To further investigate the subcellular localization of the respective proteins, NoxA, NoxB, NoxR, and PlsA were tagged with GFP and expressed under their native promoters, and the fusion constructs were ectopically integrated into the genome. NoxA was tagged either at the N- or the C-terminus in two independent strains, and both variants exhibited similar localization patterns (Fig. 4A; Fig. S3). The protein localized to the cytoplasmic membrane of vegetative hyphae but was never detected at the membrane of mature traps. Strong fluorescent signals were frequently observed in vacuoles or diffuse in the cytoplasm, which may indicate overexpression-induced degradation. The Δ*noxA* phenotype was complemented using a C-terminal GFP fusion construct, which successfully restored the wild-type phenotype.

In contrast, N-terminally tagged NoxB localized to the inner membrane of traps in vesicle-like structures (Fig. 4B). No change in localization was observed when a nematode was captured. When tagged at the C-terminus, NoxB accumulated in most traps only in one or two compartments, likely corresponding to the early trap-forming cells (Fig. 4C). A strong cytoplasmic signal, possibly originating from the endoplasmic reticulum, was also observed when tagged C-terminally. These observations suggest that the first two trap cells actively produce NoxB and display trap-specific characteristics, whereas the distal cell, which reconnects with the vegetative hypha, may transit back to a non-trap identity. Notably, only the N-terminal GFP fusion of NoxB was able to complement the Δ*noxB* phenotype. In contrast, the C-terminal GFP fusion construct failed to restore nematode capture, indicating that the C-terminal tag renders the protein non-functional.

NoxR predominantly localized to the tips of growing hyphae, forming a crescent-shaped pattern (Fig. 4D). In traps, NoxR was also detected at the trap tips. A slight increase in fluorescence was observed in the first trap compartments compared to vegetative hyphae. The presence of NoxR at the tip of trap cells together with the described phenotype suggested a role in cell-to-cell communication prior to hyphal fusion.

PlsA, a tetraspanin known to interact with NoxB, similarly localized to the inner rim of traps in vesicle-like structures (Fig. 4E). The Δ*plsA* complementation was done with the C-terminal GFP fusion construct. Co-localization analyses confirmed that PlsA and NoxB accumulate at the same subcellular positions (Fig. 4F). Notably, both proteins displayed stronger fluorescence signals in the first trap cell than in the trap cell that subsequently fuses with the basal hypha.

NoxR is oscillating at the hyphal tip

Given that the deletion of *noxR* resulted in a fusion-deficient phenotype and considering its distinct localization at the hyphal tip, we monitored NoxR in growing vegetative hyphae both in the absence of a fusion partner (monolog) and in the presence of a fusion partner (dialog) (Movies S4 and S5). In solitary hyphae, the NoxR signal indeed oscillated over time. When two hyphae approached each other for fusion, the signal

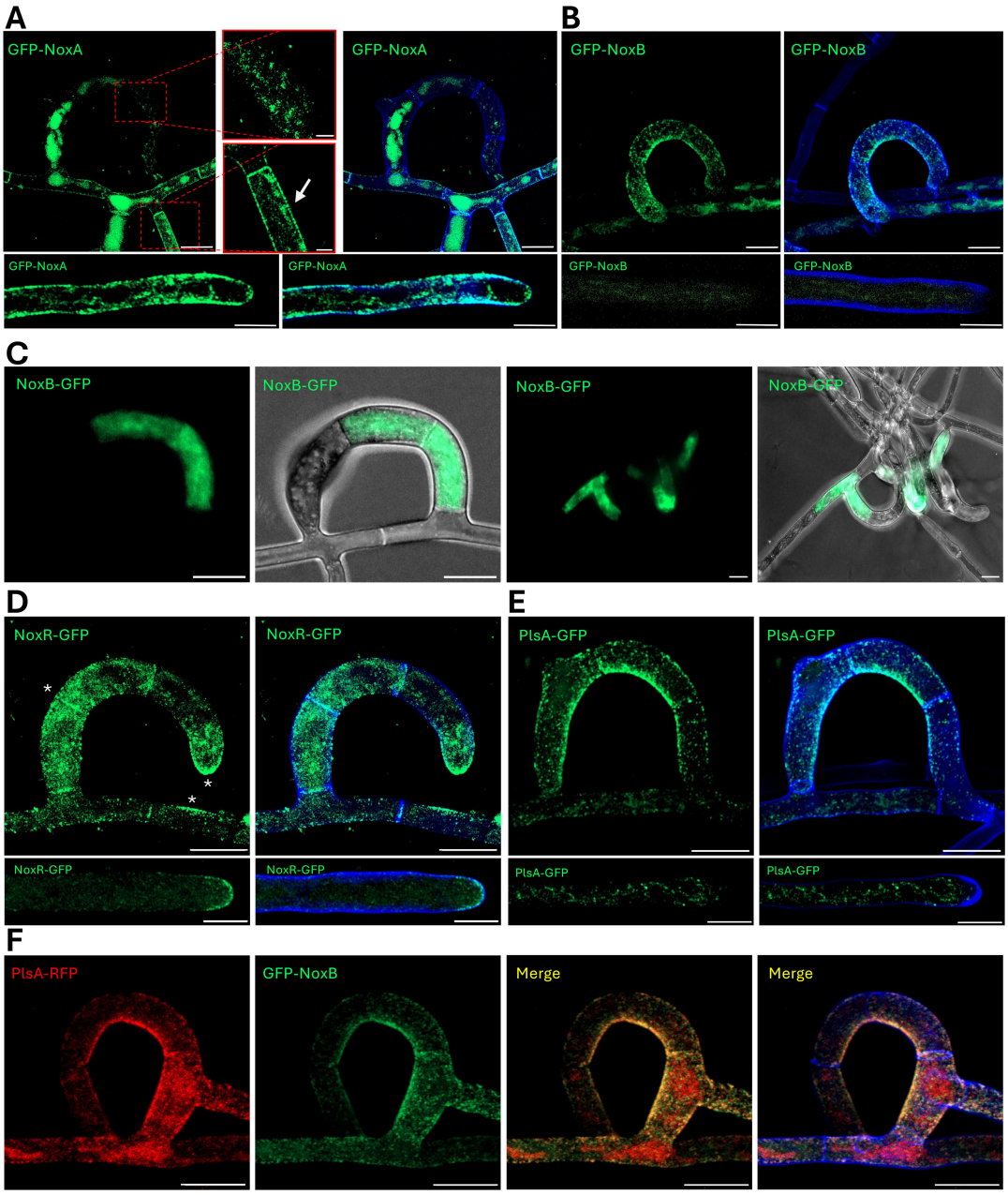

FIG 4 The NoxA complex localizes to the membrane of hyphae, whereas the NoxB complex resides at the inner rim of traps. (A) GFP-NoxA localized to the plasma membrane of vegetative hyphae and to vacuole-like compartments. In traps, plasma membrane localization was not detectable. (B, C) N-terminal and C-terminal GFP fusions of NoxB displayed distinct localization patterns. GFP-NoxB localized to vesicle-like structures at the inner rim of traps, whereas NoxB-GFP was restricted to the first two trap compartments with strong intracellular accumulation. Only the N-terminal GFP fusion is functional. (D) NoxR-GFP localized in a crescent-like pattern at the tips of growing hyphae. During trap formation, enhanced intracellular signals were observed in the first trap compartments. (E, F) PlsA-GFP showed a localization pattern similar to NoxB, forming dot-like structures at the inner rim of traps. Co-localization revealed overlapping signals. Scale bar trap: 10 µm. Scale bar hyphae: 5 µm. Scale bar NoxA magnification: 2 µm.

oscillated alternately between the two fusion partners (Fig. 5A and D). To quantify the oscillation period, seven hyphae were analyzed in monolog (n = 20 oscillation cycles) and six hyphae in dialog (n = 37 oscillation cycles) conditions, revealing that the oscillation period in dialog was slightly shorter with 124 (±21) seconds compared to the monolog with 142 (±18) seconds (Fig. 5B and C). These results suggest rhythmic interaction and activation of NoxA at the tip of hyphae.

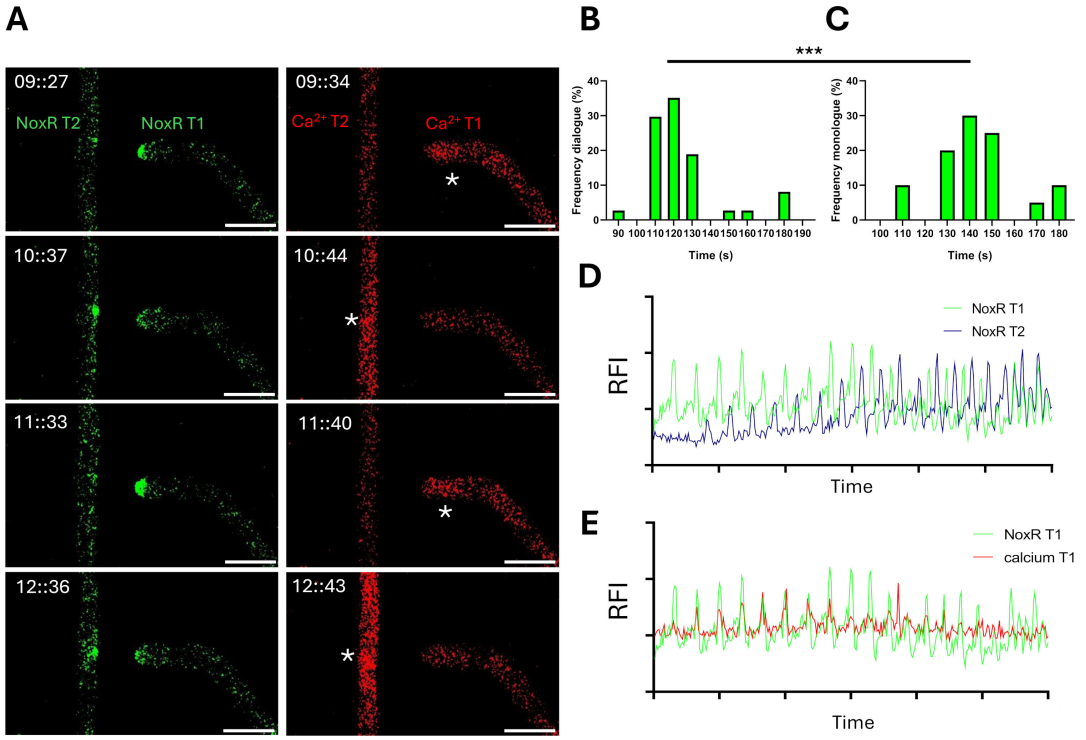

FIG 5 Oscillatory dynamics of NoxR and Ca^{2+} signaling. (A) Time-lapse imaging showing oscillatory recruitment of NoxR-GFP and intracellular calcium levels (R-GECO) during hyphal fusion. Asterisks indicate calcium spikes in the respective hyphae. Calcium spikes occurred shortly after peaks in NoxR fluorescence. Scale bar = 5 µm. (B, C) Frequency distribution of NoxR oscillations during interactions with a fusion partner (dialog, *n* = 37 oscillation cycles) or in the absence of a partner (monolog, *n* = 20). Oscillation period was shorter in the absence of a fusion partner. (D) Fluorescence intensity profiles of NoxR in two fusing hyphae (NoxR T1 and NoxR T2), revealing antiphasic oscillations. (E) Fluorescence intensity of calcium (R-GECO) and NoxR within the same hyphae during fusion, showing frequent temporal overlap of signal peaks.

These observations led us to hypothesize that hydrogen peroxide production itself might oscillate, similar to the oscillatory interplay between calcium and ROS described in plant root hairs (49). We attempted to visualize ROS using CellROX Orange; however, staining predominantly highlighted intracellular, mitochondria-associated ROS. We therefore tested OxyBURST Green H2HFF-BSA, a dye previously used in plant root hairs, but this approach did not yield a clear signal in *A. flagrans* (10). In plants, calcium and ROS oscillate within a similar temporal framework, with calcium peaks typically preceding ROS maxima (49). Calcium oscillations have also been reported during hyphal fusion in *A. flagrans* (45). To place NoxR oscillations within this broader signaling context, we analyzed calcium dynamics simultaneously with NoxR localization (Fig. 5E). To visualize calcium concentrations, the genetically encoded calcium sensor R-GECO was used (45, 50). In growing hyphae, calcium signals were generally weaker and less clearly oscillatory than the NoxR signal in monolog and dialog conditions. Nevertheless, in many hyphae, calcium and NoxR oscillations appeared to occur in a similar phase, although calcium peaks often seemed to lag slightly behind the NoxR peaks.

DISCUSSION

In eukaryotic systems, NADPH oxidases are key regulators of redox-dependent signaling and play essential roles in processes ranging from cell growth to pathogenicity. In fungi, Nox proteins are involved in sexual spore differentiation, hyphal fusion, mutualistic interactions, and virulence (14, 17, 25). In *A. flagrans*, we found that Nox proteins exhibit functional specializations that reflect the unique lifestyle of nematode-trapping species.

In contrast to many fungal systems in which both Nox isoforms contribute to virulence, in *A. flagrans* only NoxB appears to be required for the functionality of the

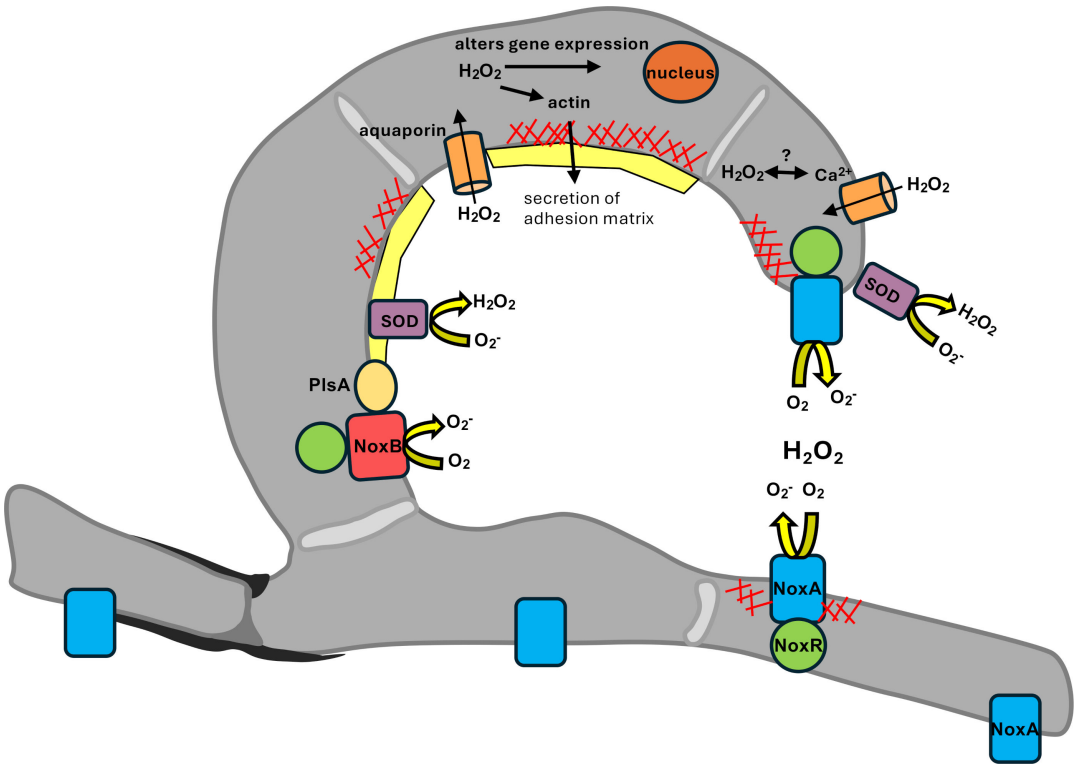

FIG 6 Model of Nox functioning during trap formation in *A. flagrans*. NoxA localizes to vegetative hyphae and to the tips of trap hyphae, where it is activated by NoxR to generate ROS. A superoxide dismutase with a putative signal peptide (SOD; DFL_005675) may contribute to the conversion of O_2^- to H_2O_2, although superoxide can also undergo spontaneous dismutation to form H_2O_2. We propose H_2O_2 as a signaling molecule. However, ROS may also facilitate actin remodeling at hyphal tips, enabling secretion of an unknown signaling molecule required for hyphal fusion. In contrast, NoxB interacts with PlsA at the plasma membrane at the inner rim of traps and is likewise activated by NoxR. This activity likely promotes secretion of the adhesive extracellular matrix that confers trap stickiness and transcriptional changes critical for virulence.

traps (21–24). This is strongly supported by expression and localization data and the phenotype of the *noxB*-deletion strain. While *noxA* was downregulated during trap induction in response to nematodes, *noxB* was upregulated together with its interaction partner *plsA*. NoxA predominantly localized to vegetative hyphae and was less detectable in traps. In contrast, NoxB localized to the inner rim of the traps and co-localized with PlsA. NoxR also showed slightly stronger fluorescence in traps compared to vegetative hyphae. These observations align with the phenotypes of the respective deletion strains: NoxB, PlsA, and NoxR are required to promote trap adhesion, whereas NoxA together with NoxR is specifically required for hyphal fusion and trap closure. The ROS generated by these enzymes may re-enter the producing cell but also the target cells through aquaporins and modulate a variety of as-yet unidentified intracellular targets in both trap cells and hyphal tips (Fig. 6).

The mechanistic basis of reduced trap adhesion in the Δ*noxB* strain remains unresolved. RNA-seq analysis did not identify any downregulated candidate adhesive proteins, although the large number of uncharacterized fungal proteins leaves open the possibility that a relevant factor did not appear in the enrichment lists. Given the known links between ROS signaling and cytoskeletal regulation in other systems, one possibility is that NoxB regulates actin dynamics in trap cells to promote secretion of the adhesive matrix (24, 51).

NoxA, in contrast, may regulate actin at the growing hyphal tip, where secretion of cell-wall-modifying enzymes or molecules for cell-cell communication is required. However, our results suggest a direct role of ROS as a signaling molecule, which raises the question about the interplay between ROS and calcium signaling. In *V. dahliae*, it

has been demonstrated that PlsA and NoxB modulate calcium levels within infection structures, and disruptions in this signaling pathway lead to reduced virulence (23). A mechanistic link between Nox and calcium signaling was established via the RAS-GAP scaffold protein IQGAP, which interacts with Ham-6 and participates in calcium-mediated processes (52). It is highly probable that similar calcium signaling cascades are involved in the regulation of both hyphal fusion and virulence in *A. flagrans*. Oscillations of ROS production are well documented in plant root hairs, where RBOH activity oscillates with calcium fluctuations to generate a feedback loop controlling polarized growth (10). This mechanism relies on calcium-activated EF-hand domains in RBOH proteins and possibly the opening of calcium channels in response to ROS (53). Such oscillations influence actin dynamics, secretion, and cell-wall remodeling (49). Although calcium oscillations are well-documented in fungal hyphae, evidence for tip-localized ROS oscillations remained elusive (54). The observed oscillation of NoxR in the current study is now strong evidence that ROS oscillations occur at the tip of growing hyphae. Whether ROS serves as a signaling molecule during hyphal fusion remains a subject of debate. We identified a putative copper-only superoxide dismutase-encoding gene in the genome of *A. flagrans*. The enzyme could convert ROS to H_2O_2. Due to their inherent unspecificity and high reactivity, ROS have been questioned as primary signaling molecules (47). Evidence from *Sordaria macrospora* supports the role of Nox proteins as upstream regulators, as their deletion leads to the significant deregulation of key communication genes (55). Since ROS are well-established as long-distance signal mediators in various systems, they remain a compelling candidate for an information molecule (11, 12). Furthermore, recent studies have demonstrated the existence of unspecific communication between different fungal species (56). Consequently, a nonspecific molecule like ROS could work together with a specific peptide to regulate this communication process. Another possibility is that ROS produced by NoxA and NoxR at the hyphal tip regulates the secretion of diffusible signaling molecules. In this case, both Nox proteins would share an effect on secretion.

To determine the precise role of ROS oscillations in fungal polarized growth and hyphal fusion, future studies should directly resolve ROS dynamics and examine their potential coupling with calcium oscillations and downstream signaling networks.

MATERIALS AND METHODS

Strains and culture conditions

A. flagrans was cultivated on potato dextrose agar (PDA) at 28°C. All *A. flagrans* strains used in this study, derived from CBS349.94, are listed in Table 1. Transgenic strains of *A. flagrans* were generated by protoplast transformation (30). The *Caenorhabditis elegans* N2 strain was obtained from Prof. Dr. Ralf Baumeister (University of Freiburg) and cultured following the protocol described in WormBook (https://doi.org/10.1895/wormbook.1.101.1).

Plasmids and strain constructions

For plasmid cloning, competent *Escherichia coli* TOP10 cells were used. All plasmids and primers in this study are listed in Tables 2 and 3. Localization studies using GFP or RFP were performed via ectopic integration of the respective plasmids into the genome.

For plasmid construction, the native promoter, open reading frame (ORF), and GFP or mCherry were cloned into the pJET1.2 backbone, together with a hygromycin (*hph*) or neomycin (*neo*) resistance cassette, using Gibson assembly. Deletion strains were generated via homologous recombination. One-kilobase fragments corresponding to the 5′ and 3′ flanking regions were amplified, and an *hph* cassette was inserted between them via Gibson assembly into pJET1.2. Successful homologous recombination was confirmed by Southern blot analysis.

For the complementation of *noxB*, the *hph* cassette in the N-terminal GFP constructs was replaced with a *neo* cassette. A similar approach was used for C-terminal localization

TABLE 1 *A. flagrans* strains used in this study

Strain	Description	Reference
WT	CBS 349.94	CBS-KNAW
sVW10	*h2b(p)::h2b::GFP*; *gpdA(p)::neo::trpC(t)*	(57)
sMK63	*noxA::hph (ΔnoxA)*; *trpC(p)::hph::trpC(t)*	This study
sMK64	*noxB::hph (ΔnoxB)*; *trpC(p)::hph::trpC(t)*	This study
sMK65	*noxR::hph (ΔnoxR)*; *trpC(p)::hph::trpC(t)*	This study
sMK66	*plsA::hph (ΔplsA)*; *trpC(p)::hph::trpC(t)*	This study
sMK67	*ΔnoxR*; *noxR(p)::noxR::noxR(t)*; *gpdA(p)::neo::trpC(t)*	This study
sMK68	*ΔnoxA*; *noxA(p)::noxA::gfp::gluC(t)*; *gpdA(p)::neo::trpC(t)*	This study
sMK69	*ΔnoxB*; *noxB(p)::gfp::noxB::gluC(t)*; *gpdA(p)::neo::trpC(t)*	This study
sMK70	*ΔnoxB*; *noxB(p)::noxB::gfp::gluC(t)*; *gpdA(p)::neo::trpC(t)*	This study
sMK71	*ΔplsA*; *plsA(p)::plsA::gfp::gluC(t)*; *gpdA(p)::neo::trpC(t)*	This study
sMK72	*h2b(p)::h2b::mCherry::tub(t)*; *noxA(p)::h2b::mCherry::tub(t)*; *trpC(p)::hph::trpC(t)*; *gpdA(p)::neo::trpC(t)*	This study
sMK73	*h2b(p)::h2b::mCherry::tub(t)*; *noxB(p)::h2b::mCherry::tub(t)*; *trpC(p)::hph::trpC(t)*; *gpdA(p)::neo::trpC(t)*	This study
sMK75	*h2b(p)::h2b::mCherry::tub(t)*; *noxR(p)::h2b::mCherry::tub(t)*; *trpC(p)::hph::trpC(t)*; *gpdA(p)::neo::trpC(t)*	This study
sMK76	*h2b(p)::h2b::mCherry::tub(t)*; *plsA(p)::h2b::mCherry::tub(t)*; *trpC(p)::hph::trpC(t)*; *gpdA(p)::neo::trpC(t)*	This study
sMK77	*noxR(p)::noxR::gfp::gluC(t)*; *trpC(p)::hph::trpC(t)*	This study
sMK78	*noxR(p)::noxR::gfp::gluC(t)*; *trpC(p)::hph::trpC(t)*; *h2b(p)::r-GECO::gluC(t)*; *gpdA(p)::neo::trpC(t)*	This study
sMK79	*noxA(p)::gfp::noxA::gluC(t)*; *trpC(p)::hph::trpC(t)*	This study
sMK80	*cdc10(p)::cdc10::mCherry::gluC(t)*; *gpdA(p)::neo::trpC(t)*	This study
sMK81	*ΔnoxB*; *cdc10(p)::cdc10::mCherry::gluC(t)*; *gpdA(p)::neo::trpC(t)*	This study

of NoxA and PlsA. For the complementation of *noxR*, the ORF, along with 1 kb of 5′ and 3′ flanking sequences, was cloned into pJET1.2 together with a neo cassette.

Microscopy and trap induction

For microscopy, fungal strains were inoculated on slides with LNM (1 g/L KCl, 0.2 g $MgSO_4 \cdot 7H_2O$, 0.4 mg $MnSO_4 \cdot 4H_2O$, 0.88 mg $ZnSO_4 \cdot 7H_2O$, 3 mg $FeCl_3 \cdot 6H_2O$, 15 g agar, pH 5.5). Spores were placed on 2 × 2 cm agar pads and incubated at 28°C for 12–24 h in darkness. For the induction of traps, around 2,000 *C. elegans* nematodes were added to the LNA agar slides. Trap counting was performed in triplicate, using three separate agar slides, each with a counted area of 0.5 cm^2.

Live cell imaging of *A. flagrans* was performed using a confocal microscope (Airyscan LSM900, Zeiss, Germany) with a 63× NA 1.4 oil objective lens (DIC M27). Time series were acquired with a gallium arsenide phosphide photomultiplier tube (GaAsP-PMT) detector, using 488 or 561 nm excitation. Differential interference contrast (DIC) images were captured on a Zeiss AxioImager Z.1 equipped with an AxioCam MR.

For NBT staining, 100 µL of a 0.5% NBT solution was added to an LNM agar slide and incubated at room temperature in the dark.

Nematode trapping assay

To evaluate trap efficiency, WT and deletion strains were inoculated on LNM as described in "Microscopy and trap induction." After 24 h, the agar pads were washed with sterile water to remove nematodes as thoroughly as possible. Small agar pieces (0.25 cm^2) were then excised, and the number of traps was counted. Approximately 150 synchronized L4-stage nematodes were added to the fungal samples. Time-lapse imaging was performed for 30 min using a Zeiss Axio Zoom.V16, and traps capturing L4 nematodes were quantified.

TABLE 2 Plasmids used in this study

Name	Description	Reference
pVW125	*h2b(p)::r-GECO::gluC(t); gpdA(p)::neo::trpC(t)*	(45)
pMK23	*plsA(p)::h2b::mCherry::tub(t); trpC(p)::hph::trpC(t)*	This study
pMK25	*plsA::hph (ΔplsA); trpC(p)::hph::trpC(t)*	This study
pMK27	*plsA(p)::plsA::gfp::gluC(t); trpC(p)::hph::trpC(t)*	This study
pMK63	*noxA::hph (ΔnoxA); trpC(p)::hph::trpC(t)*	This study
pMK64	*noxB::hph (ΔnoxB); trpC(p)::hph::trpC(t)*	This study
pMK65	*noxR::hph (ΔnoxR); trpC(p)::hph::trpC(t)*	This study
pMK67	*noxR(p)::noxR::noxR(t); gpdA(p)::neo::trpC(t)*	This study
pMK68	*noxA(p)::noxA::gfp::gluC(t); gpdA(p)::neo::trpC(t)*	This study
pMK69	*noxB(p)::gfp::noxB::gluC(t); gpdA(p)::neo::trpC(t)*	This study
pMK70	*noxB(p)::noxB::gfp::gluC(t); gpdA(p)::neo::trpC(t)*	This study
pMK71	*plsA(p)::plsA::gfp::gluC(t); gpdA(p)::neo::trpC(t)*	This study
pMK72	*noxA(p)::h2b::mCherry::tub(t); trpC(p)::hph::trpC(t)*	This study
pMK73	*noxB(p)::h2b::mCherry::tub(t); trpC(p)::hph::trpC(t)*	This study
pMK75	*noxR(p)::h2b::mCherry::tub(t); trpC(p)::hph::trpC(t)*	This study
pMK77	*noxR(p)::noxR::gfp::gluC(t); trpC(p)::hph::trpC(t)*	This study
pMK78	*noxA(p)::gfp::noxA::gluC(t); trpC(p)::hph::trpC(t)*	This study
pMK79	*cdc10(p)::cdc10::mCherry::gluC(t); gpdA(p)::neo::trpC(t)*	This study

Southern blot

To verify the deletion of the *noxA*, *noxB*, *noxR,* and *plsA* genes, a Southern blot analysis was conducted. For gDNA extraction, the fungus was inoculated in 6 cm Petri dishes with potato dextrose broth and incubated for 48 h at 28°C. The gDNA extraction followed a standard protocol (58). The gDNA of the WT and the respective deletion strains were collected and digested with an appropriate restriction enzyme overnight. The analysis followed standard protocols.

RNA extraction and quantitative RT-PCR

For RNA extraction, 10^6 *A. flagrans* spores were plated on cellophane-covered LNM plates and incubated at 28°C for 24 h. Nematodes were then added to the fungal culture, and after an additional 24 h of incubation, the mycelium was harvested and immediately frozen in liquid nitrogen. Total RNA was extracted using the E.Z.N.A. Fungal RNA Mini Kit (Omega Bio-Tek), followed by DNA digestion using the TURBO DNA-free Kit (Invitrogen).

RT-qPCR was performed using the Luna Universal One-Step RT-qPCR Kit (NEB) on a CFX Connect Real-Time PCR Detection System (Bio-Rad). Reactions were carried out in a total volume of 20 µL containing 0.2 µM of each oligonucleotide and 50 ng of RNA. The *h2b* gene served as the housekeeping reference. Each experiment included three biological replicates and three technical replicates.

The RNA sequencing was performed by BGI (Hong Kong, China). For each strain, RNA from three nematode-induced biological replicates was pooled and submitted for sequencing.

Statistical analysis

Unless otherwise stated, experiments were performed in triplicate. *P* values were calculated using an unpaired *t*-test in GraphPad Prism 9. Data presented in column graphs or scatter plots represent the mean ± standard deviation (SD), as specified in the figure legends. *P* values are indicated as follows: $*P < 0.05$, $**P < 0.01$, $***P < 0.001$, $****P < 0.0001$.

TABLE 3 Oligonucleotides used in this study

Name	Sequence (5′ to 3′)	Description
NoxA-Pf-fw	TTGTAAAACGACGGCCAGTGAATTCATGCAGGTCGAGTTACGTC	*noxA* promoter fusion
NoxA-Pf-rev	TTTCGGCGGCGGCTTTTGGTGGCATCTTGGCGGTATATCCCAGA	*noxA* promoter fusion
NoxA-GFP-fw	ATGCTCTTTCCCTAAACTCCCCCCAATGCAGGTCGAGTTACGTC	NoxA-GFP
NoxA-GFP-rev	GATTACTTACCTCACCCTTGGAAACGAAGTGTTCTTTCCAGAAGGA	NoxA-GFP
NoxA-GFP-Nter-Pro-1-fw	ATGCTCTTTCCCTAAACTCCCCCCAATGCAGGTCGAGTTACGTC	GFP-NoxA
NoxA-GFP-Nter-Pro-2-rev	TACTTACCTCACCCTTGGAAACCATCTTGGCGGTATATCCCAGA	GFP-NoxA
NoxA-GFP-Nter-GFP-3-fw	TCGCCATCTGGGATATACCGCCAAGATGGTTTCCAAGGGTGAGGT	GFP-NoxA
NoxA-GFP-Nter-GFP-4-rev	TCGACTCTTGTTTATCTGCTGCCATAGCGGCCGCTTTGTAAAGT	GFP-NoxA
NoxA-GFP-Nter-Orf-5-fw	GGATGAACTTTACAAAGCGGCCGCTATGGCAGCAGATAAACAAGAGT	GFP-NoxA
NoxA-GFP-Nter-Orf-6-rev	TAATCATACATCTTATCTACATACGCTAGAAGTGTTCTTTCCAGAAG	GFP-NoxA
NoxA-lb-fw	GATGGCTCGAGTTTTTCAGCAAGATGACAAGAAACAAATTTGTGCCAAA	Deletion *noxA*
NoxA-lb-rev	GTTGACCTCCACTAGCATTACACTTCTTGGCGGTATATCCCAGAT	Deletion *noxA*
NoxA-rb-fw	ATGCTCTTTCCCTAAACTCCCCCCAGAAAAAAAAAAATAAAAATAATCTTT	Deletion *noxA*
NoxA-rb-rev	ATTGTAGGAGATCTTCTAGAAAGATCGCAATTTGTGTTGTTGA	Deletion *noxA*
NoxA-re-GFP-fw	GATGGCTCGAGTTTTTCAGCAAGATGGTATCTATTACATTGCATT	NoxA GFP complementation
NoxA-re-GFP-rev	CCGCTCGACGTAACTCGACCTGCATTGGGGGGAGTTTAGGGAAAG	NoxA GFP complementation
NoxB-Pf-fw	TTGTAAAACGACGGCCAGTGAATTCGATTATAGATACATGTTCGGTCG	*noxB* promoter fusion
NoxB-Pf-rev	AACGCAATGCAATGTAATAGATACCCTAAGCGGCCGCTTTGTAAA	*noxB* promoter fusion
Fw-NoxB-Nter-1	ATGCTCTTTCCCTAAACTCCCCCCAGATTATAGATACATGTTCGG	GFP-NoxB
Rev-NoxB-Nter-2	TACTTACCTCACCCTTGGAAACCATTGCTTCTCAGTTTCGGACCG	GFP-NoxB
Fw-NoxB-Nter-3	CAATACGGTCCGAAACTGAGAAGCAATGGTTTCCAAGGGTGAGGT	GFP-NoxB
Rev-NoxB-Nte-4	ACGAGATCGAGCTTCTCACTGGCATAGCGGCCGCTTTGTAAAGTTCATCC	GFP-NoxB
Fw-NoxB-Nter-5	GGATGAACTTTACAAAGCGGCCGCTATGCCAGTGAGAAGCTCGAT	GFP-NoxB
Rev-NoxB-Nter-6	TAATCATACATCTTATCTACATACGTCAGAAATTCTCTTTGCCCC	GFP-NoxB
tGluC-fw	CGTATGTAGATAAGATGTAT	Backbone
NoxB-lb-fw	GATGGCTCGAGTTTTTCAGCAAGATCTTCTGTATATGGCACGGCA	*noxB* deletion
NoxB-lb-rev	GTTGACCTCCACTAGCATTACACTTTGCTTCTCAGTTTCGGACCG	*noxB* deletion
NoxB-rb-fw	ATGCTCTTTCCCTAAACTCCCCCCATGTGAGAATTTGGCTGCTCAAAA	*noxB* deletion
NoxB-rb-rev	ATTGTAGGAGATCTTCTAGAAAGATTTGACCATGCCAGCCCCAA	*noxB* deletion
NoxR-PF-fw	TTGTAAAACGACGGCCAGTGAATTCCGAGCCTAGGTTGGACGTCC	*noxR* promoter fusion
NoxR-PF-rev	TTTCGGCGGCGGCTTTTGGTGGCATGATGATGATGTGCACTTAGT	*noxR* promoter fusion
NoxR-LB-fw	GATGGCTCGAGTTTTTCAGCAAGATTCCATCAGTATTCCCCATCG	*noxR* deletion
NoxR-LB-rev	GTTGACCTCCACTAGCATTACACTTCTAAGCGGCCGCTTTGTAAA	*noxR* deletion
NoxR-RB-fw	ATGCTCTTTCCCTAAACTCCCCCCAACACGCCGCCCTCCTAAACT	*noxR* deletion
NoxR-RB-rev	ATTGTAGGAGATCTTCTAGAAAGATCACCATTTCCCTCAATCTGC	*noxR* deletion
NoxR-GFP-fw	CAATACGGTCCGAAACTGAGAAGCAATGTCGTTAAAACAGGTGGGTT	NoxR-GFP
NoxR-GFP-rev	GATTACTTACCTCACCCTTGGAAACCGCCTCGAAGGCCCAAAT	NoxR-GFP
NoxR-re-fw	ATGCTCTTTCCCTAAACTCCCCCCA TCC ATC AGT ATT CCC CAT CG	*noxR* complementation
NoxR-re-rev	ATTGTAGGAGATCTTCTAGAAAGAT CACCATTTCCCTCAATCTGC	*noxR* complementation
Fw-PlsA-PF	TTGTAAAACGACGGCCAGTGAATTCTTCGAAAAATGTTCCTTTGGATGG	*plsA* promoter fusion
Rev-PlsA-PF	TTTCGGCGGCGGCTTTTGGTGGCATCTTGGCGGTGTTCGTGATG	*plsA* promoter fusion
Fw-HR-PlsA-lb	GATGGCTCGAGTTTTTCAGCAAGATCGGATGTTGCCCAAACTTTTC	*plsA* deletion
Rev-HR-PlsA-lb	GTTGACCTCCACTAGCATTACACTTCTTGGCGGTGTTCGTGATG	*plsA* deletion
Fw-HR-PlsA-rb	ATGCTCTTTCCCTAAACTCCCCCCAAAGAGCCTAAAGAAGTTGGAAGTT	*plsA* deletion
Rev-HR-PlsA-rb	ATTGTAGGAGATCTTCTAGAAAGATATAAGAATATCTTCGGATTGAAGGG	*plsA* deletion
PlsA-GFP-re-fw	GATGGCTCGAGTTTTTCAGCAAGATGGTATCTATTACATTGCATT	PlsA-GFP complementation
PlsA-GFP-re-rev	GGATGAAAAGTTTGGGCAACATCCGTGGGGGGAGTTTAGGGAAAG	PlsA-GFP complementation
H2B_qPCR_A.flagrans_fwd	TGAAGCAAGTCCACCCTGAT	qPCR housekeeping gene
H2B_qPCR_A.flagrans_rev	GAAGCCTCAGTAGCAACACG	qPCR housekeeping gene
NoxA-qPCR_fw2	ACAGGAAATCGAAATTTGGGTG	*noxA* qPCR
NoxA-qPCR_rev2	CCATCCGTATGCAAAGAGG	*noxA* qPCR
NoxB-qPCR-fw	GACGGCATGGTCAATCGTAT	*noxB* qPCR

(*Continued on next page*)

TABLE 3 Oligonucleotides used in this study (*Continued*)

Name	Sequence (5′ to 3′)	Description
NoxB-qPCR-rev	TTCGCCCGACGATATTTC	*noxB* qPCR
PlsA-qPCR-fw	CCAATGCTGCGGTTATGTCT	*plsA* qPCR
PlsA-qPCR-rev	CCATGGCAGTGCAGCACA	*plsA* qPCR
qPCR-NoxR-fw	ACAGGAAATCGAAATTTGGGTG	*noxR* qPCR
qPCR-NoxR-rev	AAGTAATTGTCTAGCTTCACGG	*noxR* qPCR
Fw_Nter-NoxB-res	GATGGCTCGAGTTTTTCAGCAAGATGGATCCGGTATCTATTACATTG	GFP-NoxB with neo
Rev_Nter-NoxB-res	CTCGACCGAACATGTATCTATAATCTGGGGGGAGTTTAGGGAAA	GFP-NoxB with neo
mCherry-Pls-neo-fw	CGAGAAGCGAGGATTGGGTGCCATTGTAAGCAAGGGCGAGGTAA	PlsA-mCherry
mCherry-Pls-neo-rev	TAATCATACATCTTATCTACATACGCTAAGCGGCCGCTTTGTAG	PlsA-mCherry
Cdc10-fw	ATGCTCTTTCCCTAAACTCCCCCCAAGAAGTTGAGGATATATGAT	Cdc10-mCherry
Cdc10-rev	CCTCGCCCTTGCTTACCTTAATTAAGTGACCATTCGCCTCATCTG	Cdc10-mCherry
pJet-fw	ATCTTTCTAGAAGATCTCCTACAATATTC	Backbone
pJet-rev	ATCTTGCTGAAAAACTCGAGC	Backbone
trpC_rev	TGGGGGGAGTTTAGGGAAAG	Backbone
h2b_cds_fwd	ATGCCACCAAAAGCCGCC	Backbone
Efi_bb_rev	GAATTCACTGGCCGTCGTTT	Backbone
GFP-fw	ATGGTTTCCAAGGGTGAGGT	Backbone
mCherry-fw	ATGGTAAGCAAGGGCGAGG	Backbone

ACKNOWLEDGMENTS

We thank Prof. Dr. Michael Bölker for the critical review of the manuscript.

The work was supported by the Deutsche Forschungsgemeinschaft (DFG) (Fi 459/26-1).

AUTHOR AFFILIATION

[1]Department of Microbiology, Institute for Applied Biosciences, Karlsruhe Institute of Technology (KIT)—South Campus, Karlsruhe, Germany

AUTHOR ORCIDs

Marius Kriegler http://orcid.org/0009-0004-4395-4784
Reinhard Fischer http://orcid.org/0000-0002-6704-2569

FUNDING

Funder	Grant(s)	Author(s)
Deutsche Forschungsgemeinschaft	Fi 259/26-1	Reinhard Fischer

AUTHOR CONTRIBUTIONS

Marius Kriegler, Data curation, Formal analysis, Investigation, Methodology, Validation, Visualization, Writing – original draft | Valentin Wernet, Investigation, Methodology, Validation | Satur Herrero, Investigation, Methodology | Reinhard Fischer, Data curation, Formal analysis, Funding acquisition, Project administration, Resources, Supervision, Validation, Writing – review and editing

ADDITIONAL FILES

The following material is available online.

Supplemental Material

Supplemental Figures (mBio01441-26-s0001.pdf). Figures S1 to S3.
Legends (mBio01441-26-s0002.docx). Supplemental movie legends.
Movie S1 (mBio01441-26-s0003.mp4). Nematode trapping of *A. flagrans* wild type.

Movie S2 (mBio01441-26-s0004.mp4). Nematode trapping of the *A. flagrans noxB*-deletion strain.
Movie S3 (mBio01441-26-s0005.mp4). Nematode trapping of the *A. flagrans noxB*-deletion strain recorded with lower magnification.
Movie S4 (mBio01441-26-s0006.mp4). Spatiotemporal oscillation of G-GECO and NoxR-GFP during hyphal dialog.
Movie S5 (mBio01441-26-s0007.mp4). Spatiotemporal oscillation of G-GECO and NoxR-GFP in a single-hypha monolog.

REFERENCES

1. Aguirre J, Lambeth JD. 2010. Nox enzymes from fungus to fly to fish and what they tell us about Nox function in mammals. Free Radic Biol Med 49:1342–1353. https://doi.org/10.1016/j.freeradbiomed.2010.07.027
2. Temple MD, Perrone GG, Dawes IW. 2005. Complex cellular responses to reactive oxygen species. Trends Cell Biol 15:319–326. https://doi.org/10.1016/j.tcb.2005.04.003
3. De Gara L, de Pinto MC, Tommasi F. 2003. The antioxidant systems vis-à-vis reactive oxygen species during plant–pathogen interaction. Plant Physiol Biochem 41:863–870. https://doi.org/10.1016/S0981-9428(03)00135-9
4. Hansberg W, Aguirre J. 1990. Hyperoxidant states cause microbial cell differentiation by cell isolation from dioxygen. J Theor Biol 142:201–221. https://doi.org/10.1016/s0022-5193(05)80222-x
5. Finkel T. 2003. Oxidant signals and oxidative stress. Curr Opin Cell Biol 15:247–254. https://doi.org/10.1016/s0955-0674(03)00002-4
6. Segal AW, Jones OTG. 1979. The subcellular distribution and some properties of the cytochrome b component of the microbicidal oxidase system of human neutrophils. Biochem J 182:181–188. https://doi.org/10.1042/bj1820181
7. Begum R, Thota S, Abdulkadir A, Kaur G, Bagam P, Batra S. 2022. NADPH oxidase family proteins: signaling dynamics to disease management. Cell Mol Immunol 19:660–686. https://doi.org/10.1038/s41423-022-00858-1
8. Bedard K, Krause K-H. 2007. The NOX family of ROS-generating NADPH oxidases: physiology and pathophysiology. Physiol Rev 87:245–313. https://doi.org/10.1152/physrev.00044.2005
9. Bhattacharjee S. 2012. The language of reactive oxygen species signaling in plants. J Bot 2012:1–22. https://doi.org/10.1155/2012/985298
10. Monshausen GB, Bibikova TN, Messerli MA, Shi C, Gilroy S. 2007. Oscillations in extracellular pH and reactive oxygen species modulate tip growth of *Arabidopsis* root hairs. Proc Natl Acad Sci USA 104:20996–21001. https://doi.org/10.1073/pnas.0708586104
11. Niethammer P, Grabher C, Look AT, Mitchison TJ. 2009. A tissue-scale gradient of hydrogen peroxide mediates rapid wound detection in zebrafish. Nature 459:996–999. https://doi.org/10.1038/nature08119
12. Miller G, Suzuki N, Ciftci-Yilmaz S, Mittler R. 2010. Reactive oxygen species homeostasis and signalling during drought and salinity stresses. Plant Cell Environ 33:453–467. https://doi.org/10.1111/j.1365-3040.2009.02041.x
13. Aguirre J, Ríos-Momberg M, Hewitt D, Hansberg W. 2005. Reactive oxygen species and development in microbial eukaryotes. Trends Microbiol 13:111–118. https://doi.org/10.1016/j.tim.2005.01.007
14. Takemoto D, Tanaka A, Scott B. 2007. NADPH oxidases in fungi: diverse roles of reactive oxygen species in fungal cellular differentiation. Fungal Genet Biol 44:1065–1076. https://doi.org/10.1016/j.fgb.2007.04.011
15. Takemoto D, Tanaka A, Scott B. 2006. A p67Phox-like regulator is recruited to control hyphal branching in a fungal–grass mutualistic symbiosis. Plant Cell 18:2807–2821. https://doi.org/10.1105/tpc.106.046169
16. Takemoto D, Kamakura S, Saikia S, Becker Y, Wrenn R, Tanaka A, Sumimoto H, Scott B. 2011. Polarity proteins Bem1 and Cdc24 are components of the filamentous fungal NADPH oxidase complex. Proc Natl Acad Sci USA 108:2861–2866. https://doi.org/10.1073/pnas.1017309108
17. Tanaka A, Takemoto D, Hyon G-S, Park P, Scott B. 2008. NoxA activation by the small GTPase RacA is required to maintain a mutualistic symbiotic association between *Epichloë festucae* and perennial ryegrass. Mol Microbiol 68:1165–1178. https://doi.org/10.1111/j.1365-2958.2008.06217.x
18. Clergeot PH, Gourgues M, Cots J, Laurans F, Latorse MP, Pepin R, Tharreau D, Notteghem JL, Lebrun MH. 2001. PLS1, a gene encoding a tetraspanin-like protein, is required for penetration of rice leaf by the fungal pathogen *Magnaporthe grisea*. Proc Natl Acad Sci USA 98:6963–6968. https://doi.org/10.1073/pnas.111132998
19. Fu C, Iyer P, Herkal A, Abdullah J, Stout A, Free SJ. 2011. Identification and characterization of genes required for cell-to-cell fusion in *Neurospora crassa*. Eukaryot Cell 10:1100–1109. https://doi.org/10.1128/EC.05003-11
20. Nowrousian M, Frank S, Koers S, Strauch P, Weitner T, Ringelberg C, Dunlap JC, Loros JJ, Kück U. 2007. The novel ER membrane protein PRO41 is essential for sexual development in the filamentous fungus *Sordaria macrospora*. Mol Microbiol 64:923–937. https://doi.org/10.1111/j.1365-2958.2007.05694.x
21. Siegmund U, Heller J, van Kan JAL, Tudzynski P. 2013. Correction: The NADPH oxidase complexes in *Botrytis cinerea*: evidence for a close association with the ER and the tetraspanin Pls1. PLoS One 8. https://doi.org/10.1371/annotation/84c258cf-4f98-43d8-a4f0-7032cba36f22
22. Vangalis V, Papaioannou IA, Markakis EA, Knop M, Typas MA. 2021. The NADPH oxidase A of *Verticillium dahliae* is essential for pathogenicity, normal development, and stress tolerance, and it interacts with yap1 to regulate redox homeostasis. J Fungi (Basel) 7:740. https://doi.org/10.3390/jof7090740
23. Zhao Y-L, Zhou T-T, Guo H-S. 2016. Hyphopodium-specific VdNoxB/VdPls1-dependent ROS-Ca2+ signaling is required for plant infection by *Verticillium dahliae*. PLOS Pathog 12:e1005793. https://doi.org/10.1371/journal.ppat.1005793
24. Ryder LS, Dagdas YF, Mentlak TA, Kershaw MJ, Thornton CR, Schuster M, Chen J, Wang Z, Talbot NJ. 2013. NADPH oxidases regulate septin-mediated cytoskeletal remodeling during plant infection by the rice blast fungus. Proc Natl Acad Sci USA 110:3179–3184. https://doi.org/10.1073/pnas.1217470110
25. Cano-Domínguez N, Alvarez-Delfín K, Hansberg W, Aguirre J. 2008. NADPH oxidases NOX-1 and NOX-2 require the regulatory subunit NOR-1 to control cell differentiation and growth in *Neurospora crassa*. Eukaryot Cell 7:1352–1361. https://doi.org/10.1128/EC.00137-08
26. Hansberg W, de Groot H, Sies H. 1993. Reactive oxygen species associated with cell differentiation in *Neurospora crassa*. Free Radic Biol Med 14:287–293. https://doi.org/10.1016/0891-5849(93)90025-p
27. Semighini CP, Harris SD. 2008. Regulation of apical dominance in *Aspergillus nidulans* hyphae by reactive oxygen species. Genetics 179:1919–1932. https://doi.org/10.1534/genetics.108.089318
28. Tanaka A, Christensen MJ, Takemoto D, Park P, Scott B. 2006. Reactive oxygen species play a role in regulating a fungus-perennial ryegrass mutualistic interaction. Plant Cell 18:1052–1066. https://doi.org/10.1105/tpc.105.039263
29. Rinnerthaler M, Büttner S, Laun P, Heeren G, Felder TK, Klinger H, Weinberger M, Stolze K, Grousl T, Hasek J, Benada O, Frydlova I, Klocker A, Simon-Nobbe B, Jansko B, Breitenbach-Koller H, Eisenberg T, Gourlay CW, Madeo F, Burhans WC, Breitenbach M. 2012. Yno1p/Aim14p, a NADPH-oxidase ortholog, controls extramitochondrial reactive oxygen species generation, apoptosis, and actin cable formation in yeast. Proc Natl Acad Sci USA 109:8658–8663. https://doi.org/10.1073/pnas.1201629109
30. Weber M, Basu S, González B, Greslehner GP, Singer S, Haskova D, Hasek J, Breitenbach M, W Gourlay C, Cullen PJ, Rinnerthaler M. 2021. Actin cytoskeleton regulation by the yeast NADPH oxidase Yno1p impacts processes controlled by MAPK pathways. Antioxidants (Basel) 10:322. https://doi.org/10.3390/antiox10020322

31. Rossi DCP, Gleason JE, Sanchez H, Schatzman SS, Culbertson EM, Johnson CJ, McNees CA, Coelho C, Nett JE, Andes DR, Cormack BP, Culotta VC. 2017. Candida albicans FRE8 encodes a member of the NADPH oxidase family that produces a burst of ROS during fungal morphogenesis. PLOS Pathog 13:e1006763. https://doi.org/10.1371/journal.ppat.1006763
32. Jiang X, Xiang M, Liu X. 2017. Nematode-trapping fungi. Microbiol Spectr 5:5. https://doi.org/10.1128/microbiolspec.funk-0022-2016
33. Youssar L, Wernet V, Hensel N, Yu X, Hildebrand H-G, Schreckenberger B, Kriegler M, Hetzer B, Frankino P, Dillin A, Fischer R. 2019. Intercellular communication is required for trap formation in the nematode-trapping fungus *Duddingtonia flagrans*. PLoS Genet 15:e1008029. https://doi.org/10.1371/journal.pgen.1008029
34. Emser J, Wernet N, Hetzer B, Wohlmann E, Fischer R. 2024. The cysteine-rich virulence factor NipA of *Arthrobotrys flagrans* interferes with cuticle integrity of *Caenorhabditis elegans*. Nat Commun 15:5795. https://doi.org/10.1038/s41467-024-50096-4
35. Wernet N, Wernet V, Fischer R. 2021. The small-secreted cysteine-rich protein CyrA is a virulence factor participating in the attack of *Caenorhabditis elegans* by *Duddingtonia flagrans*. PLoS Pathog 17:e1010028. https://doi.org/10.1371/journal.ppat.1010028
36. Emser J, Seidler L, Kovačević E, Yu K, Rudolf T, Wohlmann E, Fischer R. 2025. The Egh16-like virulence factor TrsA of the nematode-trapping fungus *Arthrobotrys flagrans* facilitates intrusion into its host *Caenorhabditis elegans*. PLoS Pathog 21:e1013370. https://doi.org/10.1371/journal.ppat.1013370
37. Yu X, Hu X, Pop M, Wernet N, Kirschhöfer F, Brenner-Weiß G, Keller J, Bunzel M, Fischer R. 2021. Fatal attraction of *Caenorhabditis elegans* to predatory fungi through 6-methyl-salicylic acid. Nat Commun 12:5462. https://doi.org/10.1038/s41467-021-25535-1
38. Hsueh Y-P, Gronquist MR, Schwarz EM, Nath RD, Lee C-H, Gharib S, Schroeder FC, Sternberg PW. 2017. Nematophagous fungus *Arthrobotrys oligospora* mimics olfactory cues of sex and food to lure its nematode prey. Elife 6:e20023. https://doi.org/10.7554/eLife.20023
39. Hu X, Hoffmann DS, Wang M, Schuhmacher L, Stroe MC, Schreckenberger B, Elstner M, Fischer R. 2024. GprC of the nematode-trapping fungus *Arthrobotrys flagrans* activates mitochondria and reprograms fungal cells for nematode hunting. Nat Microbiol 9:1752–1763. https://doi.org/10.1038/s41564-024-01731-9
40. Kuo C-Y, Tay RJ, Lin H-C, Juan S-C, Vidal-Diez de Ulzurrun G, Chang Y-C, Hoki J, Schroeder FC, Hsueh Y-P. 2024. The nematode-trapping fungus *Arthrobotrys oligospora* detects prey pheromones via G protein-coupled receptors. Nat Microbiol 9:1738–1751. https://doi.org/10.1038/s41564-024-01679-w
41. Kriegler M, Wernet V, Hetzer B, Herrero S, Wei A, Wäckerle J, Dewein I, Fischer R. 2025. Cell-end marker proteins are required for hyphal ring formation and size determination of traps in *Arthrobotrys flagrans*. J Cell Sci 138:jcs263744. https://doi.org/10.1242/jcs.263744
42. Kriegler M, Herrero S, Fischer R. 2025. Where to grow and where to go. Fungal Genet Biol 178:103983. https://doi.org/10.1016/j.fgb.2025.103983
43. Fleissner A, Leeder AC, Roca MG, Read ND, Glass NL. 2009. Oscillatory recruitment of signaling proteins to cell tips promotes coordinated behavior during cell fusion. Proc Natl Acad Sci USA 106:19387–19392. https://doi.org/10.1073/pnas.0907039106
44. Fleissner André, Simonin AR, Glass NL. 2008. Cell fusion in the filamentous fungus, *Neurospora crassa*. Methods Mol Biol 475:21–38. https://doi.org/10.1007/978-1-59745-250-2_2
45. Wernet V, Kriegler M, Kumpost V, Mikut R, Hilbert L, Fischer R. 2023. Synchronization of oscillatory growth prepares fungal hyphae for fusion. eLife 12:e83310. https://doi.org/10.7554/eLife.83310
46. Li X, Kang Y-Q, Luo Y-L, Zhang K-Q, Zou C-G, Liang L-M. 2017. The NADPH oxidase AoNoxA in *Arthrobotrys oligospora* functions as an initial factor in the infection of *Caenorhabditis elegans*. J Microbiol 55:885–891. https://doi.org/10.1007/s12275-017-7169-x
47. Fischer MS, Glass NL. 2019. Communicate and fuse: how filamentous fungi establish and maintain an interconnected mycelial network. Front Microbiol 10:619. https://doi.org/10.3389/fmicb.2019.00619
48. Egan MJ, Wang ZY, Jones MA, Smirnoff N, Talbot NJ. 2007. Generation of reactive oxygen species by fungal NADPH oxidases is required for rice blast disease. Proc Natl Acad Sci USA 104:11772–11777. https://doi.org/10.1073/pnas.0700574104
49. Tian W, Wang C, Gao Q, Li L, Luan S. 2020. Calcium spikes, waves and oscillations in plant development and biotic interactions. Nat Plants 6:750–759. https://doi.org/10.1038/s41477-020-0667-6
50. Yamada Y, Mikoshiba K. 2012. Quantitative comparison of novel GCaMP-type genetically encoded Ca2+ indicators in mammalian neurons. Front Cell Neurosci 6. https://doi.org/10.3389/fncel.2012.00041
51. Liu N, Wang W, He C, Luo H, An B, Wang Q. 2022. NADPH oxidases play a role in pathogenicity via the regulation of F-actin organization in *Colletotrichum gloeosporioides*. Front Cell Infect Microbiol 101:845133. https://doi.org/10.1111/mmi.13391
52. Marschall R, Tudzynski P. 2016. Bclqg1, a fungal IQGAP homolog, interacts with NADPH oxidase, MAP kinase and calcium signaling proteins and regulates virulence and development in *Botrytis cinerea*. Mol Microbiol 101:281–298. https://doi.org/10.1111/mmi.13391
53. Mangano S, Juárez SPD, Estevez JM. 2016. ROS regulation of polar growth in plant cells. Plant Physiol 171:1593–1605. https://doi.org/10.1104/pp.16.00191
54. Kim H-S, Czymmek KJ, Patel A, Modla S, Nohe A, Duncan R, Gilroy S, Kang S. 2012. Expression of the *Cameleon calcium* biosensor in fungi reveals distinct Ca2+ signatures associated with polarized growth, development, and pathogenesis. Fungal Genetics Biol 49:589–601. https://doi.org/10.1016/j.fgb.2012.05.011
55. Dirschnabel DE, Nowrousian M, Cano-Domínguez N, Aguirre J, Teichert I, Kück U. 2014. New insights into the roles of NADPH oxidases in sexual development and ascospore germination in *Sordaria macrospora*. Genetics 196:729–744. https://doi.org/10.1534/genetics.113.159368
56. Haj Hammadeh H, Serrano A, Wernet V, Stomberg N, Hellmeier D, Weichert M, Brandt U, Sieg B, Kanofsky K, Hehl R, Fischer R, Fleißner A. 2022. A dialogue-like cell communication mechanism is conserved in filamentous ascomycete fungi and mediates interspecies interactions. Proc Natl Acad Sci USA 119:e2112518119. https://doi.org/10.1073/pnas.2112518119
57. Wernet V, Wäckerle J, Fischer R. 2022. The STRIPAK component SipC is involved in morphology and cell-fate determination in the nematode-trapping fungus *Duddingtonia flagrans*. Genetics 220:iyab153. https://doi.org/10.1093/genetics/iyab153
58. Zhou L, Obhof T, Schneider K, Feldbrügge M, Nienhaus GU, Kämper J. 2018. Cytoplasmic transport machinery of the SPF27 homologue Num1 in *Ustilago maydis*. Sci Rep 8:3611. https://doi.org/10.1038/s41598-018-21628-y